International Journal of Adhesion & Adhesives 134 (2024) 103815

Contents lists available at ScienceDirect

International Journal of Adhesion and Adhesives

journal homepage: www.elsevier.com/locate/ijadhadh

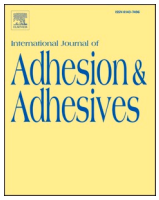

Low-temperature adhesive curing in timber engineering: About the relationship between curing kinetics and mechanical properties

Dio Lins [a,*], Steffen Franke [a], Morten Voß [b], Jonas Wirries [b]

[a] Bern University of Applied Sciences, Biel/Bienne, Switzerland
[b] Fraunhofer Institute for Manufacturing Technology and Advanced Materials IFAM, Bremen, Germany

ARTICLE INFO

Keywords:
Timber engineering
End-grain bonded timber
Low-temperature curing
Curing kinetics
Mechanical testing

ABSTRACT

Adhesive bonding plays a pivotal role in timber engineering, enhancing structural integrity, sustainability, and aesthetic appeal, while also addressing environmental concerns. The assessment of strength in adhesively bonded timber joints involves cohesive strength, adhesive strength, and substrate failure, all of which are crucial considerations for designing dependable timber structures. A comprehensive investigation was carried out with the aim of improving adhesive bonding for construction by revealing the relationship between curing progress and mechanical adhesive properties. For that, dynamic DSC measurements, kinetic modelling, tensile tests to determine the cohesive and adhesive strength, as well as tests for the evaluation of stiffness and hardness were performed using a two-component polyurethane adhesive. The investigation yielded valuable insights, particularly regarding the time- and temperature-dependent development of the curing degree and the aforementioned material properties. Additionally, the correlation between the curing degree and the respective material properties could be determined, showing that cohesion and stiffness built up occurs quite similar while the build-up of adhesive strength correlates well with hardness. It was thus concluded that Shore D hardness might represent a practical indicator for monitoring the progress of curing at low temperatures, which is a suitable means of improving adhesive applications in the construction industry.

1. Introduction

1.1. Adhesive bonding in timber engineering

Adhesive bonding plays a pivotal role in the increasing importance of timber engineering, particularly in a world marked by growing environmental concerns [1], since the technique enhances structural integrity and sustainability in timber construction. Unlike traditional fasteners, adhesives distribute stress uniformly across timber joints, bolstering load-bearing capacity and structural strength while preserving the material's integrity [2]. Furthermore, adhesive bonding provides clean and seamless joints, elevating the aesthetic appeal of timber structures, which contributes to their overall desirability. These multifaceted advantages, combined with the sustainable nature of timber, underscore the vital role of adhesive bonding in advancing timber engineering, aligning it with the world's increasing emphasis on environmentally responsible construction practices [3]. Advancements in wood adhesive bonding [4], characterised by the selection of diverse adhesives, including eco-friendly options [5], have significantly shaped the state of the art in this field [6]. These advancements have addressed environmental concerns and optimised performance [7,8]. In addition to the established timber bonding techniques, used in particular in the manufacture of engineered wood products such as glulam and cross laminated timber as well as connections like bonded-in threaded rods [4], the end-grain bonding of timber components using TS3 technology has recently become established on the market, originating in Switzerland [9]. In contrast to the above-mentioned established bonding techniques, which can usually be carried out in the factory under constant and controlled environmental conditions (temperature, humidity), TS3 bonding takes place on the construction site and is therefore exposed to environmental conditions.

1.2. Strength prediction of adhesively bonded joints

For adhesively bonded joints in timber, the assessment of strength involves a nuanced examination of at least three distinct "strengths" and associated failure modes: cohesive strength, adhesive strength, and substrates failure. Cohesive strength represents a fundamental aspect of

* Corresponding author. Bern University of Applied Sciences, Solothurnstrasse 102, 2504 Biel/Bienne, Switzerland.
E-mail address: dio.lins@bfh.ch (D. Lins).

https://doi.org/10.1016/j.ijadhadh.2024.103815
Received 22 December 2023; Received in revised form 25 June 2024; Accepted 15 August 2024
Available online 16 August 2024

adhesive bonding, characterising the intrinsic strength of the adhesive material itself. It essentially measures the adhesive's ability to maintain its structural integrity under stress. Adhesive strength, on the other hand, centres around the interface between the adhesive and the timber surfaces it adheres to. It is primarily influenced by the wood characteristics (species, density, moisture content) and condition of the surfaces to be bonded, including factors such as surface roughness and cleanliness. Adhesive strength [10] is therefore crucial for ensuring a robust and enduring bond between timber components [11]. Extensive research has been conducted to explore the multifarious factors affecting adhesive strength in timber bonding, leading to the development of techniques and treatments to enhance this critical property, for example freshly planed surfaces or application of primers. Substrate failure, the major failure mode in timber bonding, predominantly depends on the mechanical properties and characteristics of the timber materials being joined [12]. Understanding how different wood species, grain orientations, and moisture content levels influence failure of wooden substrates is paramount for designing and engineering reliable timber structures [13].

1.3. Curing kinetics of adhesives

The curing process of adhesives represents another significant aspect of timber bonding. During this phase, adhesive transits from a liquid state to a solid polymer, and the kinetics governing this transformation, referred to as curing kinetics, have been extensively studied and well-documented in the literature. While mechanical metrics such as strength or stiffness seem the most logical choice to quantify the progress of curing in engineering, it is enthalpy, typically determined using differential scanning calorimetry (DSC), that is most frequently used to express the degree of curing, α [14,15]. DSC measures the heat flow associated with chemical polymerisation of adhesives. As the adhesive cures, it undergoes exothermic or endothermic reactions, releasing or compensating heat. DSC monitors these heat changes, providing insights into the adhesive's curing process, including reaction rates, $d\alpha/dt$, thus the kinetics of polymerisation or cross-linking. Importantly, curing kinetics are highly temperature-dependent and can rely on a form of Arrhenius's law [16]. Depending upon the type of adhesive, researchers have developed several analytical expressions to model the kinetics [17], with the autocatalytic model of Kamal-Sourour [18] standing out as one of the most widely accepted and applied in the field.

1.4. Curing kinetics and low temperature curing

It is important to acknowledge that if curing kinetics is described in terms of enthalpy, the conclusions drawn thereof allow neither for predictions in terms of stiffness, nor strength, with curing time. There is still only limited experimental evidence relating the enthalpy-related curing degree to adhesive strength or stiffness, and almost no theoretical models, exist. Moussa et al. [19] investigated the mechanical properties (Young's modulus and tensile strength, referred to as stiffness and strength) of a commercial 2C epoxy cured under temperatures ranging from 5 to 20 °C. They confirmed that higher curing temperatures led to faster increases in strength and stiffness, while lower temperatures caused delays, especially in the initial curing stage. The variability of the measured strengths and stiffnesses was highest when the mechanical property curves had steep slopes but decreased with longer curing durations. The relationship between strength and stiffness, and curing time, was characterised as being sigmoidal (and approximated by a logistic function) for both metrics; that between strength and stiffness, however, was found to be almost linear for the specific epoxy considered. Ratsch et al. [20], investigating three epoxies and one polyurethane, all 2C-adhesives, suggested a non-linear, sigmoidal, relationship between the adhesive's curing degree and lap shear strength. Most lap-shear strength build-up (on aluminium substrates with cohesive failure) occurred in a limited range of curing degrees, which depended upon the adhesive considered (≈0.6–0.8 for the epoxies, and ≈0.5–0.6 for the polyurethane). These results, completed by other studies, e.g. by Wirries et al. [21], indicate that, as for strength, stiffness build-up also occurs relatively suddenly in a relatively narrow range of curing degrees. Complementing the aforesaid, it is important to underscore that irrespective of the curing conditions, whether at low temperatures or via hot/post-curing techniques, comparable mechanical properties, including maximum strength and failure strain, are attained for fully cured adhesives [22].

Shore hardness testing, akin to various hardness tests, assesses the indentation depth in the material caused by a specified force applied by a standardised presser foot. This depth relied on the material's hardness, viscoelastic characteristics, and the presser foot's shape [23]. Gent [24] or Qi et al. [25] have derived a relationship between ASTM D2240 hardness and Young's modulus for elastomers using linear elastic indentation hardness. Therefore, Shore hardness can serve as a quick and uncomplicated substitute for Young's modulus, offering a convenient in-situ measurement during the curing process without the need for intricate adhesive sample testing. Understanding the changing Shore hardness over time and during curing is thus a convenient proxy of adhesive behaviour, even though it frequently received limited research focus.

1.5. Scope of this article

This study aims to fill the knowledge gaps highlighted above by conducting a thorough investigation into how low-temperature curing affects the tensile strength and stiffness of a 2C-PUR adhesive itself (cohesive) as well as the tensile strength of end-grain bonded timber and how these properties evolve over time. Besides standard mechanical and thermomechanical characterisation, Shore hardness, a practical in-situ measurement method during curing, will serve as a valuable proxy for the adhesive's curing behaviour. A further novelty of this study is the comprehensive investigation of the correlation between the predicted curing degrees (as determined by thermomechanical analysis) and the respective mechanical properties.

Ultimately, the research will contribute to making adhesive bonding more suitable for construction, particularly during colder months when low-temperature curing is essential. The development of predictive models for early-age properties under varying curing conditions will advance timber engineering practices and provide valuable guidance for construction decisions. The scientific roadmap of the publication has been illustrated in Fig. 1.

2. Materials & methods

2.1. Materials

The materials that were analysed are precisely those that are used for the end-grain bonding of timber components with TS3 technology, as described in Chapter 1. The adhesive used is a two-component polyurethane, more precisely TS3's proprietary casting resin "TS3 PTS CR192″, which has been developed for end-grain bonding of timber components. This adhesive is manufactured without the addition of solvents and formaldehyde and the most important characteristics of the adhesive can be found in Table 1.

For all timber specimens spruce timber of strength class T14/C24 according to DIN EN 338:2016 [26] was used. The test specimen had a cross section of 10 × 20 mm and were 400 mm long. To isolate the influence of temperature, all other potential factors affecting tensile strength were minimised as much as possible. This involved a clearly defined density of 350 kg/m^3 with a low variation of ±25 kg/m^3 achieved through manual selection. Additionally, a wood moisture content of 12 % was targeted for all test series. This was achieved by adjusting relative humidity according to the respective temperature conditions to attain a wood moisture equilibrium at 12 % following Keylwerth and

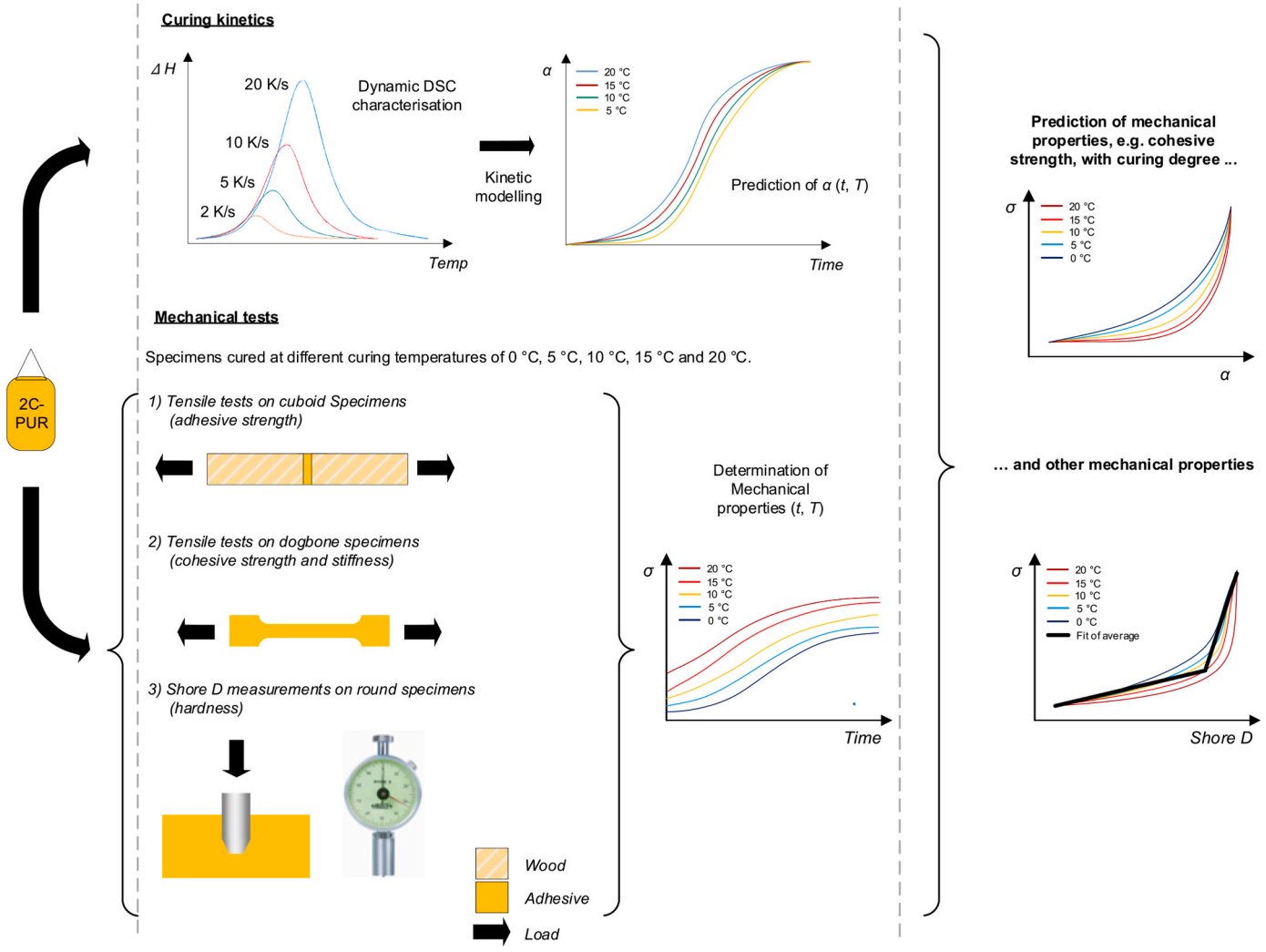

Fig. 1. Scientific roadmap.

Table 1
Essential material characteristics taken from manufacturer's technical data sheet (TDS) as well as values marked with * that have been measured. Curing times marked with ** calculated based upon Arrhenius law [15]. All values valid for RT-cured adhesive formulations.

Characteristic	TS3 PTS CR192
Adhesive type	2C-PUR
Density, ρ [g/cm^3]	1.32
Pot life for curing at +23 °C [min]	30
Curing time at +23 °C [h]	240
Curing time at +5 °C [h]	480**
Curing time at −10 °C [h]	1920**
Initial viscosity at RT, η [Pa·s]	1.5–4.5
Polymerisation enthalpy H_{Total} [J/g]	149.5 ± 5.5
Modulus of elasticity, E [MPa]	≈1000
Tensile strength, σ_u [MPa]	≈45
Elongation at break, ε_u [%]	≈5
Lap shear strength, τ_u, on spruce [MPa]	8.1 ± 0.6*

Noack [27]. Wood defects, particularly knots, which significantly affect the tensile strength of small test specimens bonded at their end-grain have also been excluded.

2.2. DSC measurements and kinetic modelling of the adhesive

Dynamic DSC measurements were conducted using a Discovery DSC from TA Instruments with varying heating rates (2, 5, 10 and 20 K/min) after calibration against the melting point of an indium sample to ensure precise temperature readings. The adhesive was mixed manually according to TDS guidelines and quickly prepared within a 10-min window, well within their pot life, ensuring substantial chemical curing within the DSC.

Measurements occurred within a temperature range of 0 °C–250 °C. Each measurement cycle included cooling samples to 0 °C, holding the temperature for 1 min to establish thermal equilibrium, and subsequently heating them to 250 °C with an additional 1-min hold. To confirm complete curing, samples underwent a second identical curing cycle immediately after the first heating program. Heat flow was measured over time and compared to an empty sample receptacle to determine heat generated during adhesive curing.

Kinetic modelling employed the software Kinetics Neo® (Netzsch-Gerätebau GmbH, Germany), utilising data from the DSC curing cycles of all five measurements. For the two-component adhesive, a model-based analysis featuring the Kamal and Sourour kinetic model [18] with a single reaction step was employed to enable prediction of the curing degree over time and temperature.

2.3. Tests for cohesive strength

The strength of the adhesive was assessed in accordance with SN EN ISO 527–1:2020 and SN EN ISO 527–2:2012. Test specimens were produced by pouring the adhesive into silicone moulds to achieve the desired geometry. Immediately after casting, the test specimens, along with the casting device, were placed in a climate chamber at the respective temperatures (0°–20 °C, in 5 °C steps, see Table 2). On the first day of testing, all test specimens from a series were removed from the mould, and their thickness was calibrated to the specified 4 ± 0.2 mm using a wide belt sander (grit 100). Subsequently, the test specimens were returned immediately to the environment and retrieved at the designated times for tensile testing (see Table 2). Tests were conducted within a timeframe of less than 15 min following retrieval from the climatic chamber, with the aim of minimising any potential effects stemming from the adhesive curing at room temperature.

In addition to cohesive strength, the tests also allowed for the determination of the adhesive stiffness, expressed herein as the Young's, or elastic, modulus, which was defined as the slope of the σ-ε-curve in the strain-range between 0.0 and 0.1 %. All tensile tests were conducted with a loading rate of 2 mm/min under constant conditions of 20 °C and 65 % relative humidity. Given the homogeneity of the adhesive following the mixing of its two components and the expectation of low variation, only three test specimens were assessed per testing day and temperature.

2.4. Tests for adhesive strength on wood

Samples were manufactured in close alignment with the standards outlined in SN EN 301:2018 and SN EN 302–1:2013. For the preparation of end-grain bonded timber joints, laminated timber elements were initially crafted from seven spruce board lamellas, each with a length of about 0.4 m. This process resulted in the creation of structural glulam blocks distinguished by a consistent alignment of annual rings. These glulam blocks were then split once again in the middle. The surfaces to be bonded later were pre-treated with a higher viscosity variant of the adhesive that was also used for bonding. Then both parts were joined together at room temperature with a 4 mm adhesive layer thickness. The potting process was carried out by injection through a filling orifice positioned at the centre of the outer lamella; injection was performed from bottom to top so to avoid the formation of air bubbles.

Following the casting of the adhesive, one of these glulam blocks was placed in the respective climate chamber for each temperature test. On the first day of testing, the laminated timber elements were further dissected, resulting in test specimens measuring 10 × 20 mm, as shown in Figs. 2 and 3. These freshly created specimens were once again situated within the climate chamber and subjected to testing on specific days (see Table 2). The end-grain bonded timber joints underwent testing within a maximum of 30 min after the removal of the test specimens from the climate chamber. Despite the various approaches undertaken to homogenise timber properties, it was still presumed that timber, and consequently, the end-grain bonded timber joints, exhibited greater variability, if compared to casting resin. Consequently, to ensure statistical significance, five test specimens were scrutinised for each test

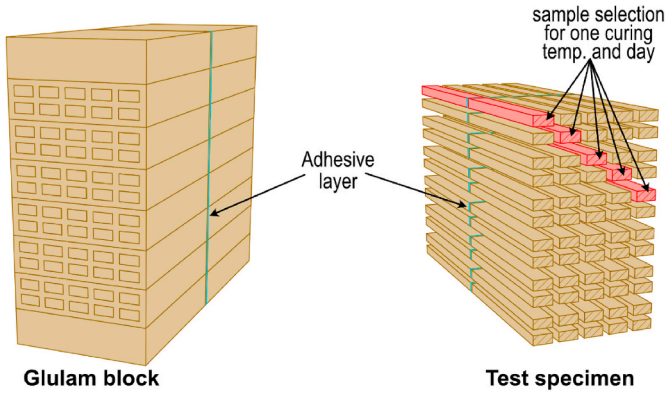

Fig. 2. Principal illustration of the manufacturing of the end-grain/butt joints used to assess development of adhesive strength.

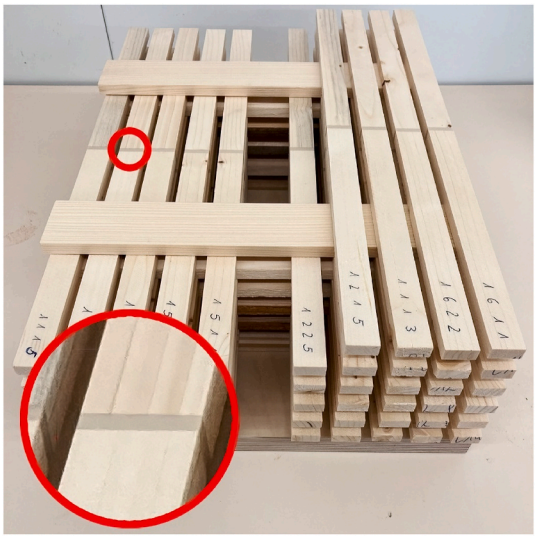

Fig. 3. A set of butt-joints after conditioning.

day and temperature to ensure the robustness of the results. These were originating from distinct raw lamellae and various locations within the Glulam block (see Fig. 2). The complexity of this test specimen production process was driven by the necessity to eliminate potential edge-related influences, such as bubble formation or incomplete casting. While these factors are generally inconsequential on a larger component scale, they can lead to notable variations in the geometry of small test specimens.

The tensile tests were conducted in accordance with SN EN 408+A1:2012 along with SN EN 14080, Annex E2:2013 using a vertical tensile testing machine (Zwick 20 kN, cf. Fig. 4). The test specimens were designed with a free length of approximately 200 mm per side. They were executed at a constant standard climate of 20 °C and 65 %

Table 2
Experimental programme, all specimens tested at 20 °C and 65 % r.h.

	Cohesive strength/Young's modulus	Adhesive strength	Shore hardness
Curing temperatures [°C]		0; 5; 10; 15; 20	
Testing times [days]		1; 2; 3; 6; 10; 15; 20; 30	
Quantity per day and temperature	3	5	5
Testing speed	2 mm/min	2 mm/min	15 s/measurement
Standards	SN EN ISO 527–1:2020 SN EN ISO 527–2:2012	SN EN 408+A1:2012 SN EN 14080, Annex E2:2013	SN EN ISO 868:2003

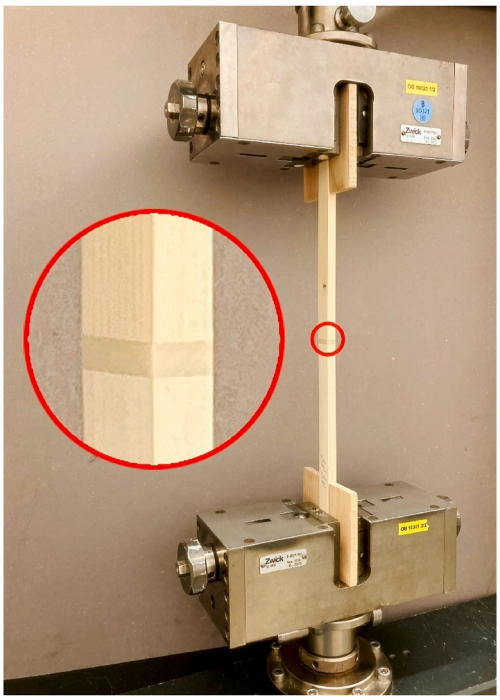

Fig. 4. Testing of one butt-joint to assess adhesive strength on spruce timber (*Picea Abies*).

relative humidity, resulting in an unchanged wood moisture equilibrium at 12 %. The climate was recorded continuously with a corresponding data logger (ALMEMO 2470 1SCRH). The tensile tests were carried out at a displacement-controlled test speed of 2 mm/min.

2.5. Hardness test

The samples used for this study consisted of small round plates with a diameter of about 10 cm. These plates were cast in appropriately designed moulds and then placed in the climatic chamber together with the tensile specimens. To measure the Shore D hardness, a durometer according to SN EN ISO 868:2003 was used. The durometer was pressed on the sample for 15 s and then the result could be read off. The tests were carried out at 20 °C and 65 % relative humidity. For every test day and temperature, a total of five hardness measurements were performed on distinct samples, as shown in Fig. 5.

Fig. 5. Shore D hardness measurement performed on an adhesive sample.

2.6. Experimental programme

To provide a clear overview of the previously discussed experiments, the following table shows the experimental programme conducted in detail.

3. Results

3.1. Kinetic modelling

The findings from the DSC measurements carried out following the appropriate heating regimen have been depicted in Fig. 6-a. These graphs serve to underscore the precision of the kinetic models employed. The Kamal-Sourour model displayed a good correlation with the empirical data, achieving a r^2 value of 0.997.

Given the strong concordance between the experimental data and the model fit, it is now possible to predict the extent of conversion for any arbitrary curing cycle of the adhesive material. Therefore, the prediction of the degree of cure for isothermal curing was performed at temperatures between 0 °C and 20 °C in 5 °C steps, as tested in the experiments. These predictions are presented in Fig. 6-b. Overall, it can be concluded that most of the curing process takes place between 1 h and 2 days, and that higher temperatures, as expected, lead to a faster development of the degree of cure.

3.2. Material properties in function of time

3.2.1. Cohesive strength

The term cohesive tensile strength is defined in the following as being the failure load of the dog-bone-shaped adhesive samples, divided by the cross-section; width and thickness thereof have been determined for each individual sample using a calibrated calliper. The cohesive strength displayed a consistent pattern of enhancement over time, irrespective of the curing temperature considered, as shown in Fig. 7-a. Notably, at lower temperatures, specifically 0 °C, a prolonged duration of almost two weeks was necessary to attain significant tensile strengths. It was evident that temperature played a pivotal role in expediting the development of cohesive strength.

When cured at 15 °C, a mere 2 days were sufficient for the adhesive to reach 25 MPa, whereas achieving the same level of strength at 0 °C demanded nearly 3 weeks. For curing temperatures of 15 °C and 20 °C, the strengthening process plateaued after approximately one week of curing, with no noteworthy increases observed thereafter. Conversely, in the case of lower temperatures, such as 0 °C and 5 °C, the final strength of the 20 °C series remained unattained even after an extensive month-long curing period. This variance in strength development underscores the critical influence of temperature on the adhesive curing process. It can also be observed that the curing speed at 0 °C is initially relatively slow, increasing significantly after approximately three days and reaching a plateau after four weeks, after which it remains constant. Conversely, the initially low curing speed at 20 °C is not discernible on the logarithmic time axis, as this has evidently risen sharply after just a few hours.

3.2.2. Adhesive strength

The butt-jointed spruce boards systematically failed at the adhesive-timber interface in a pure adhesive failure mode, for which Fig. 8 stands as a representative depiction. In the following evaluation, strength is evaluated as being the failure load (F_{max}) divided by the cross-section of the timber board a × b, whose dimensions were measured for each individual sample using a calibrated calliper.

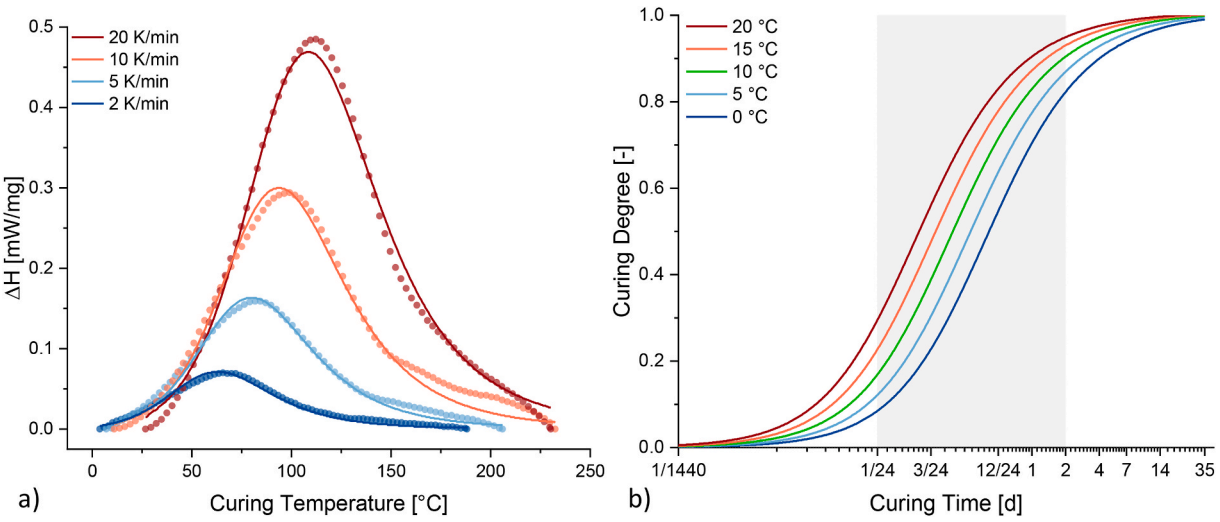

Fig. 6. Thermo-mechanical analysis of the adhesive with a) DSC results and b) development of curing degree.

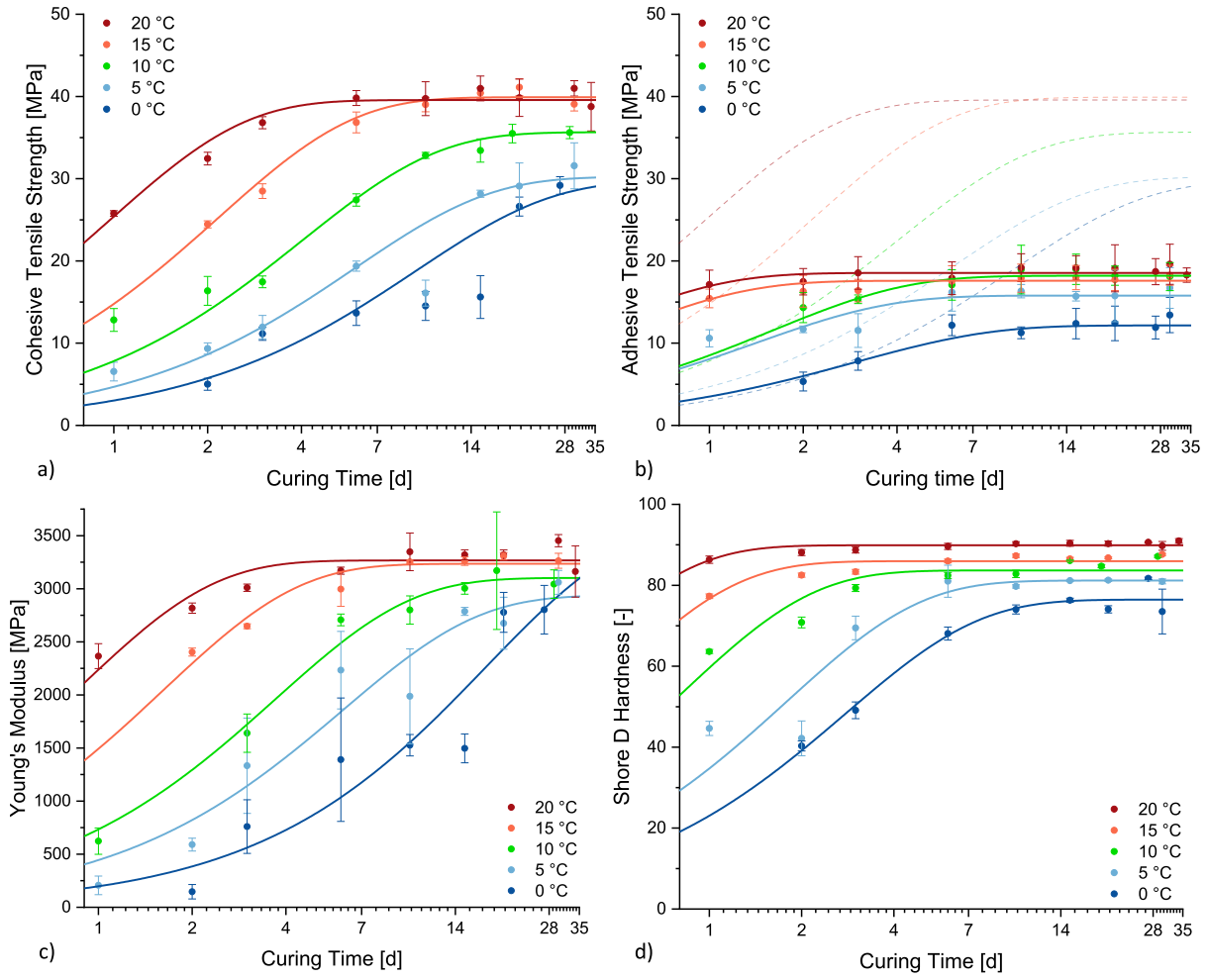

Fig. 7. Evolution of material properties with time: cohesive strength (a), adhesive strength (b), Young's modulus (c) and Shore D hardness (d); all trendlines added for the discussion.

The adhesive strength, as assessed through tests conducted on spruce, demonstrated a pattern distinct from that observed in cohesive strength, as illustrated in Fig. 7-b. Particularly at lower temperatures, notably 0 °C, there was a discernible increase in adhesive strength within approximately 14 days, culminating in a final value of approximately 10 MPa. Similarly, when cured at 5 °C, a gradual rise in adhesive strength occurred, elevating it from roughly 10 MPa to around 15 MPa. However, as the curing temperature increased, the evolution of adhesive

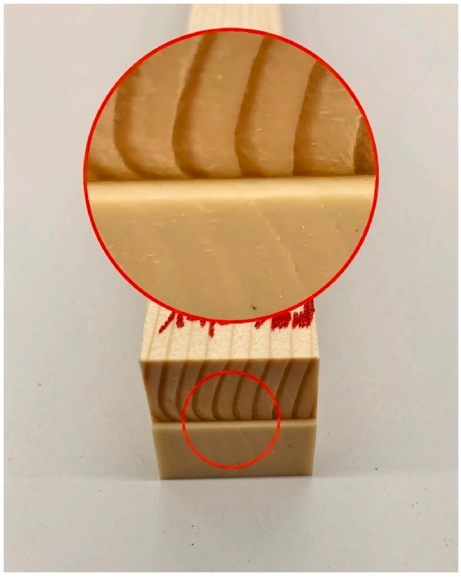

Fig. 8. Representative adhesive failure mode observed for the butt-joints.

strength showed a progressively flatter tendency with curing time. Notably, once a curing temperature of 10 °C was exceeded, there were almost no discernible differences in the adhesive strength's development. This observation highlights the influence of curing temperature on adhesive strength, with lower temperatures promoting more distinct increases, while higher temperatures resulted in a plateauing effect in the strength evolution. At a curing temperature of 20 °C, final strength is achieved in a mere of two days. In contrast, at 0 °C, the maximum strength is only attained after two weeks. At 0 °C, strength is approximately one-third lower than at 20 °C.

3.2.3. Young's modulus

The intrinsic stiffness of the adhesive, as expressed by its *E*-modulus reported in Fig. 7-c, was observed to be increased over time for all the considered curing temperatures. However, it was strongly dependent on the latter. When cured at the lowest temperature of 0 °C, an almost complete build-up of stiffness required about 5 weeks, whereas at 20 °C, this was achieved within a span of 4–5 days. Seven days after curing at 0 °C, E was found to be approximately 1200 MPa, while at 5 °C, E was about 2000 MPa. At 10 °C, E reached roughly 2600 MPa, and at 15 °C, E was around 3200 MPa. Finally, at 20 °C, it attained its almost final value, with E almost being equal to 3200 MPa. It was noted that the data indicated that the evolution of stiffness resulted in curves being shifted by similar time offsets when plotted on a logarithmic scale. Additionally, it was important to observe that the scatter in the experimental data increased as the curing temperatures decreased. It is also noteworthy that the difference in initial stiffness, i.e. after one day of curing, is approximately 10 times higher at 20 °C than at 0 °C. Conversely, equivalent values are attained after approximately five weeks, irrespective of the curing temperature.

3.2.4. Shore hardness

Shore hardness measurements revealed a more intricate pattern of results depicted in Fig. 7-d. Adhesives cured at lower temperatures exhibited a clear and consistent increase in Shore hardness over the course of curing. This trend was also observed for adhesives cured at 5 °C and 10 °C, although it was notably less pronounced compared to the lower temperatures. In stark contrast, adhesives cured at 15 °C and higher temperatures nearly instantly displayed their ultimate Shore hardness values, with only marginal, if any, further increases observed as the curing time extended. This distinctive behaviour underscores how Shore hardness is influenced by curing temperature, with lower temperatures leading to a more gradual increase. Regardless of the curing temperature considered, the observed scatter was found to be minimal. Additionally, the hardness after one day at 20 °C is approximately four times higher than at 0 °C. However, the final hardness, which is reached after two days at 20 °C but only after approximately ten days at 0 °C, is at the same level.

3.2.5. Fitting parameters

As suggested by the experimentally determined data regarding cohesive and adhesive strength presented in the preceding subsections, it becomes evident that temperature played the most prominent role. To allow for better quantified insights in aforesaid relations, the data resulting from the mechanical characterisation was modelled. Cohesive and adhesive strength were modelled using an exponential function so to mimic the observed trends. This function assumes that each dataset corresponding to a curing temperature converges towards a final value (σ_∞) following an exponential increase expressed by Eq. (1), in which t_1 represents a characteristic time constant at which 63 % of the final strength is achieved. Note that for each curing temperature a different set of σ_∞ and t_1 are expected. This fitting was executed utilising the software OriginPro2022.

$$\sigma(t) = \sigma_\infty \left[1 - e^{-t/t_1}\right] \tag{1}$$

The selected simple fit-function appeared to adequately model the experimental data (with r^2-values up to 0.99), as shown in the previously presented Fig. 7. It yielded, for both cohesive and adhesive strength, as well as for each considered curing temperature, a final value (σ_∞) to which the data converged, and a characteristic time (t_1) that indicated the rate at which the evolutions occurred.

Plotting the fitted parameters σ_∞ and t_1 for cohesive and adhesive strength, as done in Fig. 9, reveals the following. Firstly, cohesive strength converges to final values that lie, depending upon the curing temperature, between slightly below 30 MPa (for curing at 0 °C) to roughly 38 MPa (curing at 20 °C). This data, if plotted against the curing temperature, as done in Fig. 9-a, is well approximated by a linear fit (with a slight slope of 0.6 MPa/°C); it appears, however, to some extent legitimate to simply consider it constant (≈35 MPa). Secondly, the pace of the strength increase can be well modelled as log t_1 being linearly dependent upon the curing temperature. The resulting (negative) slope of this curve, depicted in Fig. 9-b, is $k = -0.048$ (with $r^2 = 0.97$); this means that every 5 °C reduction leads to slowing the reaction by about 43 %.

Turning the focus on adhesion strength, the same fitting procedure outlined above indicates that strength converges for all curing temperatures to the almost identical final value (of 16.5 MPa, cf. Fig. 9-c); a linear fit resulted in a very marginal increase with curing temperature of 0.2 MPa/°C. The characteristic time (t_1) appears to exhibit a relation such that log t_1 decreases linearly with curing temperature, as shown in Fig. 9-d. Here, the (negative) slope is $k = -0.043$ ($r^2 = 0.86$), which corresponds to every 5 °C reduction leads to slowing the reaction by about 40 %. Since the kinetics of cohesion and adhesion strength exhibit (very) similar slopes (differing by a mere 10 %), it appears tempting to equal them, suggesting a similar mechanism in strength formation with time.

3.3. Material properties in function of curing degree

3.3.1. Cohesive strength

When the adhesive's cohesive strength was plotted not as a function of time, as exemplified in Fig. 7-a, but in relation to the corresponding curing degree α (Fig. 9-a), several observations were made. The cohesive strength, regardless of the curing temperatures, was observed to progress relatively slowly until α reached approximately 0.7, at which point a noteworthy increase in tensile strength commenced.

On the other hand, Fig. 10-a, the correlation of the time-related

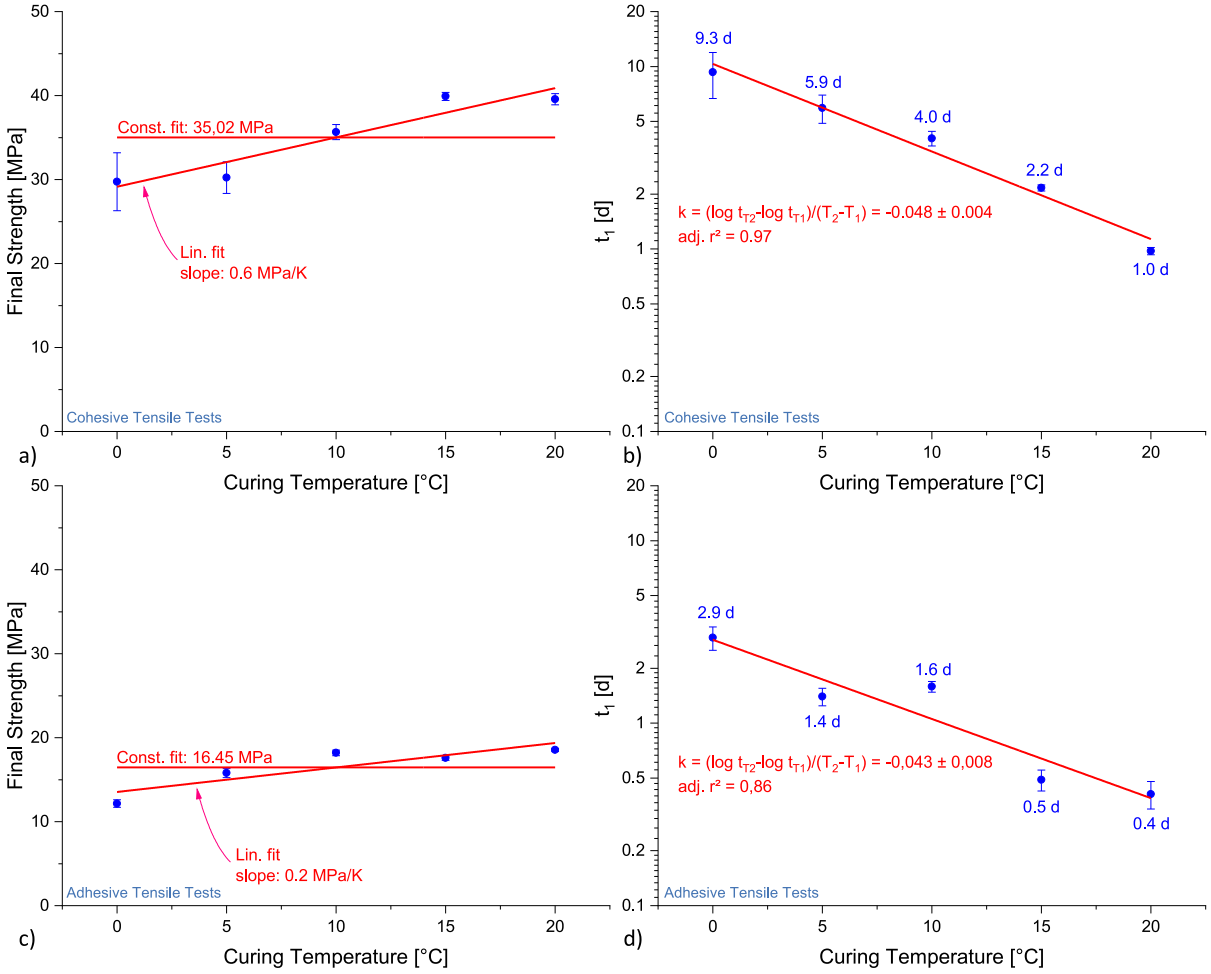

Fig. 9. Fitting parameters for cohesive (top) and adhesive strength (bottom) in function of curing temperature.

variables cohesive strength and curing degree concealed the temporal aspect, which was reintroduced into focus by overlaying time information onto the plots. This revealed that while the relationship between tensile strength and curing degree displayed some independence from curing temperature, it was underscored that time continued to play a substantial role. Notably, it required 6 h for the adhesive to achieve $\alpha \approx 0.7$ at 20 °C, whereas at 0 °C, an entire day was necessary to attain the same level of curing.

3.3.2. Adhesive strength

The adhesive strength, when charted against the curing degree α, was observed to undergo a continuous augmentation, as shown in Fig. 10-b. Nevertheless, this augmentation was found to be non-linear. More substantial increases in adhesive strength were achieved as the α-values approached the culmination of the curing process, albeit to a lesser extent when compared to cohesive tensile strength. The curves for 15 °C and 20 °C displayed a notable resemblance; as the curing temperatures decreased, the curing progress became increasingly directed towards higher α-values.

3.3.3. Young's modulus

The elastic modulus E of the adhesive exhibited a continuous increase in conjunction with the curing degree, as shown in Fig. 10-c. It was apparent that, for all curing temperatures, E tended towards a common ultimate value. In contrast to cohesive tensile strength, the increment was notably non-linear. Below a curing degree α of approximately 0.7, there was no notable development of stiffness, a threshold that was almost equivalent to $\alpha \approx 0.9$ for the lower curing temperatures of 0 °C and 5 °C. While the selected representation (strength versus curing degree) fundamentally omitted temporal information, it is noteworthy that a curing degree of 0.9 was achieved in approximately 3 days at 20 °C (corresponding to $E \approx 3250$ MPa). In the same time frame, the same adhesive only attained $E = 560$ MPa, despite possessing a similar curing degree α.

3.3.4. Shore hardness

Finally, the focus was directed towards the connection between Shore D hardness (hereinafter referred to as hardness) and the curing degree α, revealing the pattern illustrated in Fig. 10-d. Hardness exhibited a continuous increase with α in a non-linear manner. Unlike the observations made for the E-modulus, there was no specific curing degree at which the alteration in hardness increase became significant. Nevertheless, at lower curing degrees, the augmentation in hardness was notably more pronounced towards higher α-values, resulting in more skewed curves for the lower curing temperatures.

3.4. Other relationships

Based upon the information gathered so far, it was tempting to investigate potential relationships between the measured and fitted data. When adhesive strength was plotted against cohesive strength, as depicted in Fig. 11-a, it was observed that the influence of curing temperature on the relationship was minimal, except for the lowest value of 0 °C. It was evident that the value of adhesive strength was, on average,

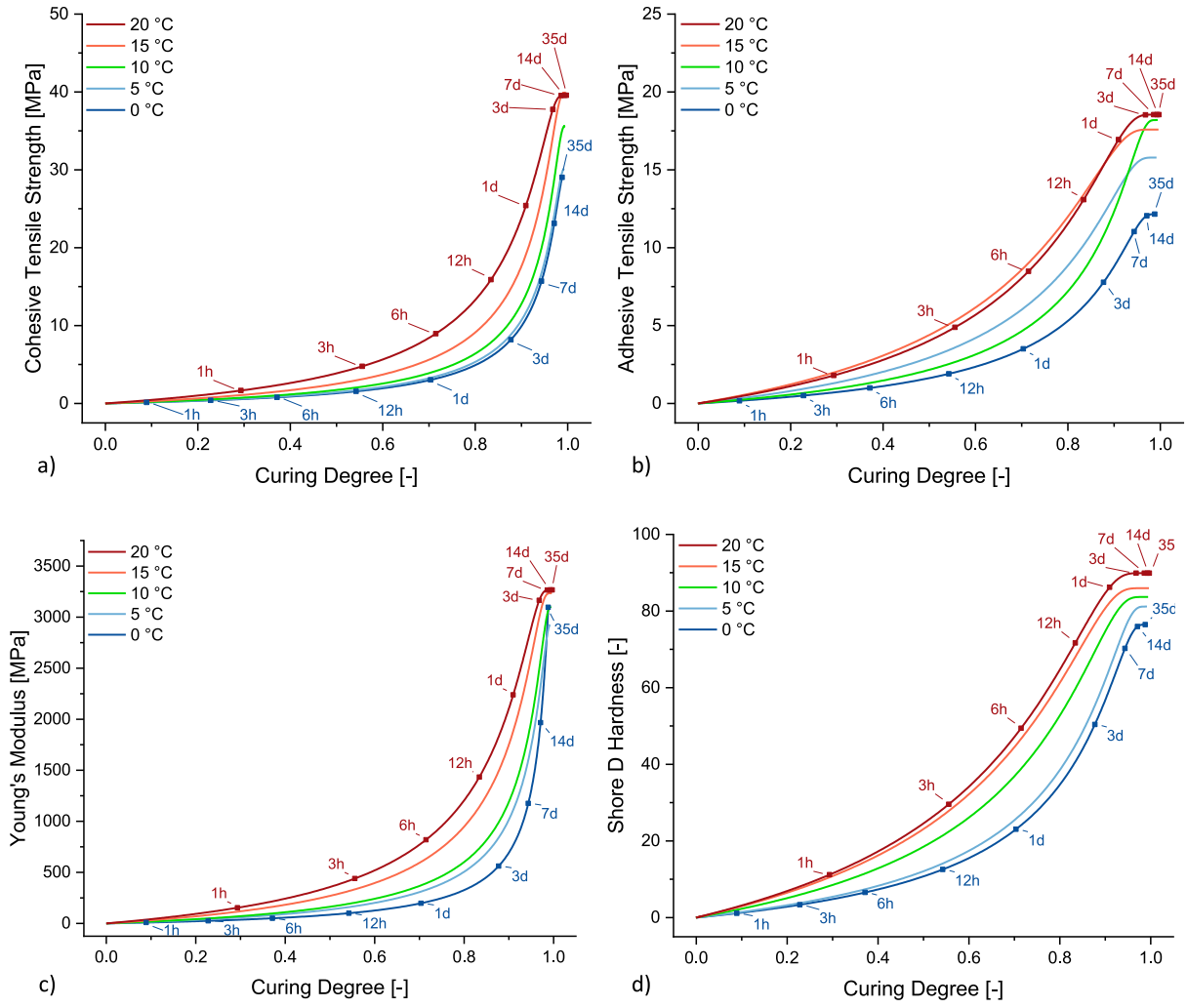

Fig. 10. Evolution of material properties with curing degree: cohesive strength (a), adhesive strength (b), Young's modulus (c) and Shore D hardness (d); all trendlines added for the discussion.

capped at 16.2 MPa. A simplification of the relationship to a bilinear one was possible, with an almost linear 1:1 correspondence up to 16.2 MPa.

It should be noted that Fig. 11-a, and all subsequent figures, omitted temporal information regarding the unfolding of cohesive and adhesive strength. To reintroduce this information, specific time intervals (1 h, one day, and seven weeks) were designated for two representative curing temperatures, namely 5 °C and 15 °C. This clearly demonstrated that although the initial (1 h) and final (35 d) stages of the curing process might seem closely aligned despite a 10 °C temperature difference, there was a distinct variation when examining the curing process at the 1-day mark.

The relationship between the adhesive's Young's modulus and Shore D hardness was illustrated in Fig. 11-b. Below Shore D hardness levels of approximately 70 (corresponding to $E \approx 1200$ MPa), there existed an almost linear correlation with the corresponding E-modulus. In this segment of the data, the curves representing different curing temperatures appeared to be ordered from highest to lowest, although the 10 °C curve deviated somewhat from this pattern. Beyond this point, there was a steep rise in E-values, and the curves reordered according to curing temperature (with 0 °C exhibiting the lowest and 20 °C the highest Shore D hardness). To some extent, the relationship could be simplified as bilinear, which would suit the needs of practitioners. In a manner like the previous observation concerning curing time, the difference between the start and end times, despite the 10 °C temperature difference, was not readily apparent. However, at the 1-day mark, it became evident that distinct stages were reached.

The cohesive strength of the adhesive and Shore D hardness, as observed in Fig. 11-c, exhibited a correlation independent of the adhesive's curing temperature. The relationship could be described as two-staged. Initially, there was a linear increase in cohesive strength up to approximately 75 Shore D hardness, reaching around 14 MPa. Subsequently, no significant changes in Shore D hardness occurred as the adhesives attained their final strength. A bilinear fit was suggested, which exhibited a kink at the aforementioned values and allowed practitioners to estimate fairly accurate values conveniently. Analogous to previous observations regarding timing, the 10 °C difference in curing temperature was not evident at the start or end of the curing process but became apparent at an intermediate stage (specifically, after 1 day).

The relationship between the adhesive strength and Shore D hardness, as illustrated in Fig. 11-d, appeared to be relatively independent of the curing temperature and exhibited a relatively linear pattern (excluding the outlier represented by 10 °C). When averaged, all resulting curves could be approximated by a linear fit, providing practitioners with a reasonably straightforward methodology to estimate adhesive strength based on direct in-situ measurements, without the need for extensive laboratory work. As previously mentioned, while the initial (1 h) and final (35 d) stages of the curing process did not seem crucial, the marked timestamp of 1 day clearly highlighted the

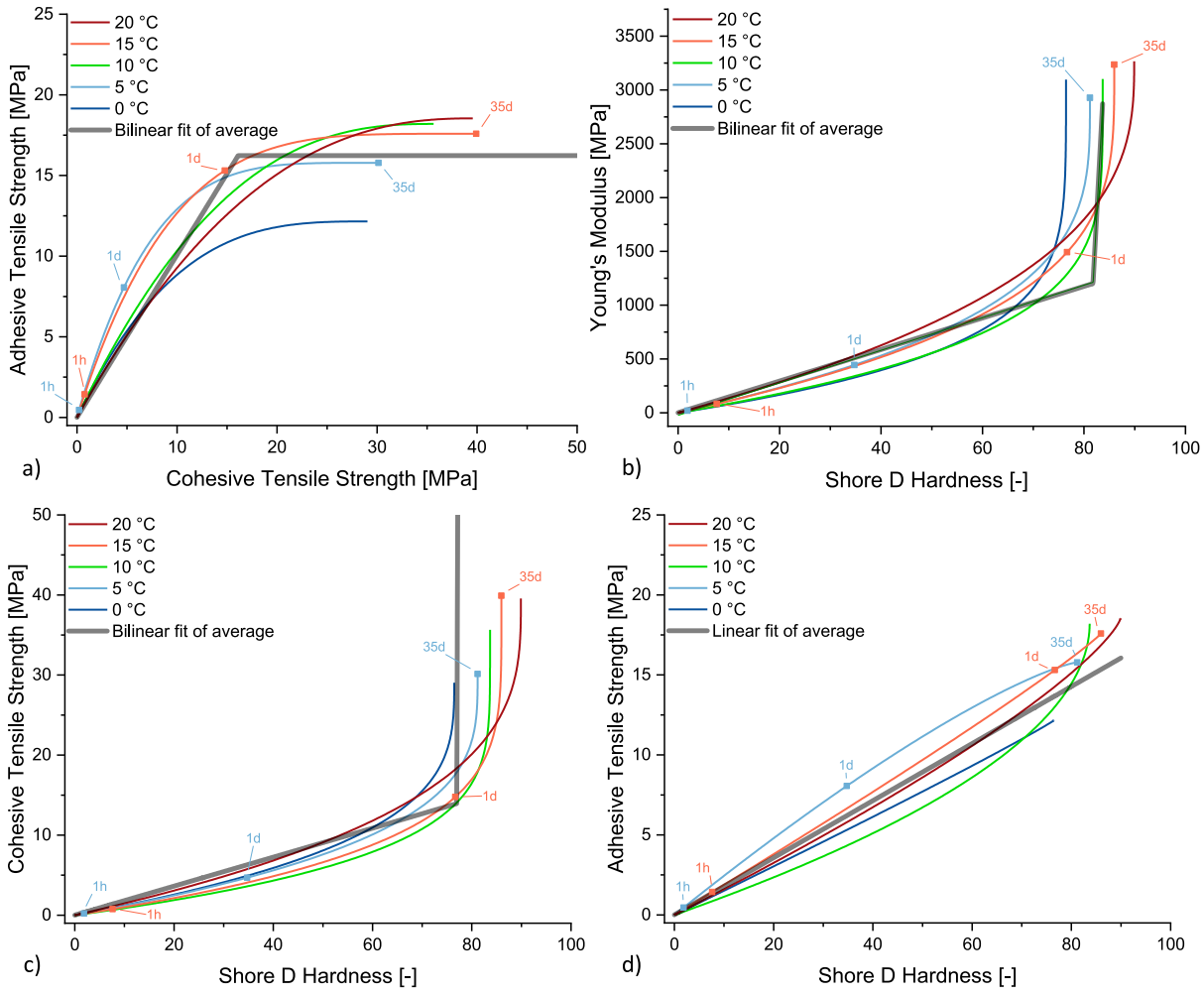

Fig. 11. Relationships between the material properties under consideration.

significant role played by the curing temperature difference.

4. Discussion

4.1. Material properties in function of time

Cohesive strength exhibited a consistent increase over time, irrespective of the curing temperature. However, the rate and duration required for this increase varied significantly with temperature. This underscored the pivotal role played by temperature in the development of cohesive strength. Nevertheless, while the final strengths measured at different temperatures vary, it is assumed that identical strengths can be achieved through further curing at 20 °C.

Adhesive strength demonstrated a different behavioural pattern. Lower curing temperatures, like 0 °C, exhibited a noticeable increase in adhesive strength within approximately 10 days, reaching a value of around 10 MPa. At 5 °C, a gradual but distinguishable rise occurred, elevating it from roughly 10 MPa to around 15 MPa. In contrast, as the curing temperature increased beyond 10 °C, the evolution of adhesive strength displayed a progressively flatter pattern, with minimal differences observed. The influence of curing temperature on adhesive strength development was apparent.

The stiffness of the adhesive increased with time across all curing temperatures, but the rate of change varied significantly. At the lowest temperature of 0 °C, it took about five weeks to achieve full stiffness, whereas at 20 °C, this was accomplished in just 4–5 days. This variation in the rate of stiffness development directly correlated with curing temperature, with lower temperatures requiring considerably more time. The respective temperature-dependent developments of the (tensile) modulus of elasticity and cohesive tensile strength exhibit a remarkable degree of concordance. This might represent an indication that the two material properties develop in a simultaneous manner within the adhesive.

The temperature-dependent temporal development of the Shore hardness exhibited a complex pattern. Lower temperatures consistently showed an increase in hardness over time. In contrast, at 15 °C and higher temperatures, the adhesives quickly reached their ultimate hardness values, with only marginal or negligible further changes as the curing time extended. Thus, the rate of hardness increase appeared to be influenced by curing temperature.

These findings collectively highlighted the substantial role of curing temperature in shaping the evolution of cohesive and adhesive strength, stiffness, and hardness over time. Lower temperatures tended to result in more gradual changes, requiring extended durations to achieve specific material properties. Conversely, higher temperatures accelerated these processes, reaching desired material properties more swiftly. Despite variations, the kinetics of cohesion and adhesion strength exhibited commonalities, hinting at a shared underlying mechanism governing strength development.

4.2. Material properties in function of curing degree

When cohesive strength was analysed concerning curing degree α, it became evident that cohesive strength progressed relatively slowly until α reached approximately 0.7. Beyond this point, a significant increase in tensile strength was observed. The exact threshold for this change remained somewhat uncertain, but it appeared to increase with decreasing curing temperatures. The relationship between tensile strength and curing degree showed a degree of independence from curing temperature. However, the influence of time remained significant. For instance, achieving $\alpha \approx 0.7$ required just 6 h at 20 °C but demanded a full day at 0 °C.

In contrast, adhesive strength exhibited continuous but non-linear growth as a function of curing degree α. The increases in adhesive strength were more pronounced as α approached the culmination of the curing process. Notably, the trends observed for curing temperatures of 15 °C and 20 °C displayed similarities, with lower temperatures directing the curing process more towards higher α-values.

The elastic modulus E of the adhesive increased continuously with curing degree, and all curing temperatures ultimately converged towards a common ultimate value. However, the increment was notably non-linear. There was minimal stiffness development below a curing degree α of approximately 0.7, and this threshold varied, being around $\alpha \approx 0.9$ for the lower curing temperatures of 0 °C and 5 °C. These observations were noteworthy, even though the selected representation, which plotted strength versus curing degree, omitted temporal information.

Shore hardness (referred to as hardness) displayed continuous but non-linear growth with curing degree α. Unlike the observations made for the E-modulus, there was no specific curing degree at which the alteration in hardness increase became significant. Nevertheless, at lower curing degrees, the increase in hardness was notably more pronounced towards higher α-values, resulting in more skewed curves for lower curing temperatures.

In summary, the relationship between material properties (cohesive strength, adhesive strength, Young's modulus, and Shore hardness) and curing degree α showcased both commonalities and variations. All properties tended to increase with α, but the rate of increase and the critical points of change varied significantly. Curing temperature consistently exerted influence, with lower temperatures often leading to more pronounced changes in material properties at lower curing degrees.

4.3. Other relationships

The impact of curing temperature on the cohesive strength-adhesive strength relationship was minimal, except at 0 °C. Adhesive strength consistently averaged around 16.2 MPa, exhibiting a bilinear relationship up to this point.

Regarding the relationship between the adhesive's Young's modulus and Shore D hardness, a nearly linear correlation existed below specific hardness and modulus levels, with temperature influencing the order of curves. Beyond this point, both hardness and modulus values increased steeply, with temperature differences becoming evident at the 1-day mark.

Conversely, the cohesive strength of the adhesive and Shore D hardness appeared relatively independent of curing temperature, featuring a two-staged relationship: an initial linear increase in cohesive strength up to specific hardness values, followed by minimal changes as the adhesives reached their final strength. A bilinear fit was suggested, facilitating convenient estimation. The 10 °C difference in curing temperature did not significantly affect the start or end of the curing process but became apparent at an intermediate stage (after 1 day). The relationship between the adhesive's Young's modulus and adhesive strength appeared relatively independent of curing temperature, displaying a relatively linear pattern when averaged. This provided practitioners with a straightforward methodology to estimate adhesive strength based on in-situ measurements without extensive laboratory work, with the influence of curing temperature being significant across these relationships.

5. Conclusion

Adhesive bonding plays a pivotal role in timber engineering, enhancing structural integrity, sustainability, and aesthetic appeal while addressing environmental concerns. Assessing strength in adhesively bonded timber joints involves cohesive strength, adhesive strength, and substrate failure, crucial for designing reliable timber structures. Curing kinetics, a fundamental aspect of adhesive bonding, are assessed using differential scanning calorimetry (DSC), with kinetics being temperature-dependent and analytical models like the Kamal-Sourour model aiding in understanding the curing process. Limited experimental evidence connects enthalpy-related curing degrees to adhesive strength and stiffness, highlighting the impact of curing temperature on strength and stiffness development.

To enhance the understanding and predictability of adhesive bonding for construction, particularly during colder months, several activities were undertaken to address knowledge gaps. Dynamic DSC measurements were conducted using a TA Instruments Discovery DSC with varying heating rates. Kinetic modelling was carried out using Kinetics Neo® software and the Kamal and Sourour kinetic model. Cohesive strength tests tensile testing assessed cohesive strength and stiffness under controlled temperature conditions. Adhesive strength examinations focused on end-grain bonding at low temperatures, in accordance with approved standards, with temperature as the primary variable and other potential factors affecting tensile strength minimised. Hardness assessments adhered to EN ISO 868 standards, utilising an appropriate durometer. Predictive models for early-age properties under varying curing conditions were also developed to advance timber engineering practices and offer valuable guidance for construction decisions. Key findings resulting from these experimental investigations include.

- Cohesive strength consistently improved over time, with a significant dependency on curing temperature. Lower temperatures required extended durations to achieve significant tensile strengths, while higher temperatures accelerated the process, reaching desired strengths more swiftly. While the final strength is achieved after around a week at 20 °C, it takes five weeks to achieve comparable cohesive strength when curing takes place at 0 °C.
- Adhesive strength displayed distinct behaviour. Lower curing temperatures led to a noticeable increase in adhesive strength within around 10 days, while higher temperatures exhibited a flatter trajectory. Compared to cohesive strength, maximum adhesive strength is reached approximately twice as quickly, i.e., after two weeks at 0 °C.
- Stiffness increased with time across all temperatures, with lower temperatures requiring considerably more time to achieve full stiffness. The development of the (tensile) Young's modulus is comparable to that of cohesive tensile strength, with both metrics reaching e.g. 60 %–70 % of their final value after two days at 15 °C.
- Shore hardness exhibited a complex pattern, increasing consistently at lower temperatures and quickly reaching ultimate values at higher temperatures. The progression of hardness is comparable to that of adhesive strength, with final hardness being reached faster compared to adhesive strength (2 d at 20 °C/14 d at 0 °C).

Finally, the study showed how a relationship between mechanical adhesive properties and the degree of curing can be achieved. It can be summarised that cohesive tensile strength and modulus of elasticity develop in a relatively short range of the curing degree, mostly between $\alpha = 0.7–0.9$. For $\alpha < 0.7$, in contrast, there is hardly any significant increase in strength or stiffness observable. The outcome of the study for

adhesive strength and Shore D hardness was different since they both progress more uniformly with the curing degree. In detail, ca. 25 %–45 % (adhesive strength) as well as about 30 %–50 % (Shore D hardness) of the final material characteristics have already been built up when α reaches 0.7.

In addition, an almost linear correlation between hardness and adhesive strength was observed, which holds true regardless of the curing temperature considered. This interesting result provides a valuable possibility of using Shore D hardness as an indicator for the curing progress of the end-grain bonding, especially when other techniques may be impractical or time-consuming. Incorporating these predictive insights into adhesive applications can lead to more efficient and tailored processes, ultimately enhancing the reliability and performance of adhesive bonds in various environmental conditions.

CRediT authorship contribution statement

Dio Lins: Writing – original draft, Visualization, Validation, Methodology, Investigation, Formal analysis, Conceptualization. **Steffen Franke:** Supervision, Funding acquisition. **Morten Voß:** Writing – review & editing. **Jonas Wirries:** Writing – review & editing.

Declaration of competing interest

The authors declare that they have no known competing financial interests or personal relationships that could have appeared to influence the work reported in this paper.

Data availability

The data that has been used is confidential.

Acknowledgement

The project represents a collaborative effort involving Timber Structures 3.0 AG, Schilliger Holz AG, Henkel & Cie. AG, ETH Zürich, and Bern University of Applied Sciences. The authors extend their sincere appreciation for the strong collaboration among the project partners. Additionally, the authors would like to express their gratitude to Innosuisse for providing significant funding support for this ongoing project [Application Number: 50393.1 IP-ENG]. Further thanks are due to the COST Action CA20139 “Holistic design of taller timber buildings” (HELEN), which funded the scientific exchange between Bern University of Applied Sciences and IFAM Bremen, resulting in this publication.

References

[1] Ramage MH, Burridge H, Busse-Wicher M, Fereday G, Reynolds T, Shah DU, et al. The wood from the trees: the use of timber in construction. Renew Sustain Energy Rev 2017;68:333–59. https://doi.org/10.1016/j.rser.2016.09.107.
[2] Dillard DA. Advances in structural adhesive bonding. second ed. Woodhead Publishing; 2023 [S.l.].
[3] Woodard AC, Milner HR. 7 - sustainability of timber and wood in construction. In: Khatib JM, editor. Sustainability of construction materials. second ed. Woodhead Publishing Series in Civil and Structural Engineering. Woodhead Publishing; 2016. p. 129–57.
[4] Vallée T, Tannert T, Fecht S. Adhesively bonded connections in the context of timber engineering – a Review. J Adhes 2017;93(4):257–87. https://doi.org/10.1080/00218464.2015.1071255.
[5] Kaufmann M, Kolbe J, Vallée T. Hardwood rods glued into softwood using environmentally sustainable adhesives. J Adhes 2018;94(11):991–1016. https://doi.org/10.1080/00218464.2017.1385459.
[6] Davis G. The performance of adhesive systems for structural timbers. Int J Adhesion Adhes 1997;17(3):247–55. https://doi.org/10.1016/S0143-7496(97)00010-9.
[7] Stoeckel F, Konnerth J, Gindl-Altmutter W. Mechanical properties of adhesives for bonding wood—a review. Int J Adhesion Adhes 2013;45:32–41. https://doi.org/10.1016/j.ijadhadh.2013.03.013.
[8] Broughton J, Hutchinson A. Adhesive systems for structural connections in timber. Int J Adhesion Adhes 2001;21(3):177–86. https://doi.org/10.1016/S0143-7496(00)00049-X.
[9] Zöllig S, Frangi A, Franke S, Muster M. Timber structures 3.0 – new technology for multi-axial, slim, high performance timber structures. World Conference on Timber Engineering 2016:1258–65. https://repositum.tuwien.at/bitstream/20.500.12708/172/2/Eberhardsteiner20Josef20-20201620-20WCTE20201620e-book20containing20all20full20papers.
[10] Basin VE, Berlin AA. Adhesive strength. Polym Mech 1970;6(2):266–71. https://doi.org/10.1007/BF00859200.
[11] Gardner DJ, Blumentritt M, Wang L, Yildirim N. Adhesion theories in wood adhesive bonding. In: Progress in adhesion and adhesives; 2015. p. 125–68.
[12] Dinwoodie JM. Timber—a review of the structure-mechanical property relationship. J Microsc 1975;104(1):3–32. https://doi.org/10.1111/j.1365-2818.1975.tb04002.x.
[13] Burmester A. Einfluß von Holzfeuchtigkeit und Rohdichte auf die Schlagbiegefestigkeit von Kiefern-, Fichten- und Buchenholz/Influence of moisture content and density on impact bending strength of spruce, pine and beech wood/L'influence de l'humidité et de la densité sur la résistance à la flexion au choc du bois de pin. d' épicéa et de hêtre 1970;12(9):313–6. https://doi.org/10.1515/mt-1970-120906.
[14] Prime RB. Differential scanning calorimetry of the epoxy cure reaction. Polym Eng Sci 1973;13(5):365–71. https://doi.org/10.1002/pen.760130508.
[15] Voß M, Vallée T. Effects of Curie particle induced accelerated curing on thermo mechanical performance of 2K structural adhesives – Part I: bulk properties. J Adhes 2022;98(9):1298–339. https://doi.org/10.1080/00218464.2021.1909482.
[16] Laidler KJ. The development of the Arrhenius equation. J Chem Educ 1984;61(6):494. https://doi.org/10.1021/ed061p494.
[17] Yousefi A, Lafleur PG, Gauvin R. Kinetic studies of thermoset cure reactions: a review. Polym Compos 1997;18(2):157–68. https://doi.org/10.1002/pc.10270.
[18] Kamal MR, Sourour S. Kinetics and thermal characterization of thermoset cure. Polym Eng Sci 1973;13(1):59–64. https://doi.org/10.1002/pen.760130110.
[19] Moussa O, Vassilopoulos AP, Castro J de, Keller T. Early-age tensile properties of structural epoxy adhesives subjected to low-temperature curing. Int J Adhesion Adhes 2012;35:9–16. https://doi.org/10.1016/j.ijadhadh.2012.01.023.
[20] Ratsch N, Böhm S, Voß M, Adam M, Wirries J, Vallée T. Accelerated curing of glued-in threaded rods by means of inductive heating – part II: modelling. J Adhes 2021;97(3):251–81. https://doi.org/10.1080/00218464.2019.1654865.
[21] Wirries J, Vallée T, Rütters M. How to predict residual stresses of curing adhesives ab initio solely using extended rheometry. J Adhes:1–37. https://doi.org/10.1080/00218464.2023.2184264.
[22] Savvilotidou M, Vassilopoulos AP, Frigione M, Keller T. Effects of aging in dry environment on physical and mechanical properties of a cold-curing structural epoxy adhesive for bridge construction. Construct Build Mater 2017;140:552–61. https://doi.org/10.1016/j.conbuildmat.2017.02.063.
[23] Tsukizoe T, Hisakado T. On the theoretical analysis of Shore hardness. Bulletin of JSME 1965;8(29):20–7. https://doi.org/10.1299/jsme1958.8.20.
[24] Gent AN. On the relation between indentation hardness and Young's modulus. Rubber Chem Technol 1958;31(4):896–906. https://doi.org/10.5254/1.3542351.
[25] Qi HJ, Joyce K, Boyce MC. Durometer hardness and the stress-strain behavior of elastomeric materials. Rubber Chem Technol 2003;76(2):419–35. https://doi.org/10.5254/1.3547752.
[26] DIN EN 338:2016-07, Bauholz für tragende Zwecke_- Festigkeitsklassen; Deutsche Fassung EN_338:2016. Berlin: Beuth Verlag GmbH. https://doi.org/10.31030/2463437.
[27] Keylwerth R, Noack D. Bundesforschungsanstalt für Forst-und Holzwirtschaft, Reinbek Institut für Holzphysik und mechanische Holztechnologie. Holz als Roh-Werkst 1964;22(1):29–36. https://doi.org/10.1007/BF02627726.